

# Measuring the Charge of an Electron through Millikan's Oil Drop Experiment

Hyun Wallace Anderson

The Ohio State University, Physics Department, Columbus, Ohio, 43210

Here we conduct Millikan's oil drop experiment in order to measure the charge of an electron. Electrically charged oil droplets are sprayed with an atomizer into a capacitor and are digitally recorded when in free-fall due to gravity and when an electric field is present. Digital video microscopy techniques, such as Crocker-Grier algorithms, are used to computationally track and measure their velocities; allowing us to calculate their charge using a derivation of Newton's second law equations. In conducting this experiment, we find that the oil droplets exhibit a variety of charges, all of which can be quantized as a factor of a single charge:  $1.47 \cdot 10^{-19}$  coulombs.

## Introduction

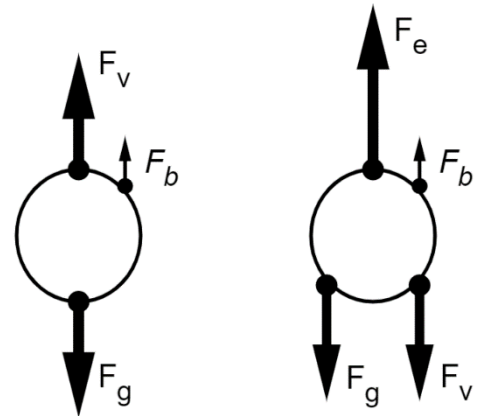
In 1909, physicist Robert A. Millikan devised the first accurate and direct measurement of a subatomic particle: the charge of an electron. He performed this experiment by spraying a mist of atomized oil particles into a capacitor and ionizing them with x-rays to give them a negative charge. By observing their velocity with and without the influence of a uniform electric field, Millikan was able to derive their size and charge by equating the Newton's second law equations which act upon them, as seen in **Fig. 1**.

Here we will reconduct Millikan's oil drop experiment using modern techniques in order to determine the charge of an electron. This is done by atomizing charged oil droplets into a capacitor and measuring their velocities using an AI tracking algorithm with and without the influence of a uniform electric field. Using this data, along with other independent variables such as barometric pressure, capacitor dimensions, and voltage will allow us to calculate the precise forces acting upon the particles, thereby giving us their radius and charge. In conducting this experiment, we found that the particles within the mist exhibit different charges, all of which can be quantized as a single electron charge:  $1.47 \cdot 10^{-19}$  coulombs.

## Theory

Stokes' law states that when a small sphere falls freely through a viscous medium, such as air, it acquires a constant velocity when the drag force comes into equilibrium with the force of gravity. At this terminal state where net forces equal zero we only require the particle's velocity as well as some environmental constants in order to derive its physical properties such as radius and charge. This relationship provides the mathematical basis of the experiment.

There are two states in which the experiment is conducted: when the particles undergo free-fall from the force of gravity and when a high voltage is applied across the capacitor plates, creating a uniform electric field around the particles: the forces acting upon the droplet in either scenario can be seen in the two free body diagrams in **Fig. 1**. These forces are detailed in equations (1) through (4), though buoyancy force  $F_b$  is neglected in further derivation as the density of oil is much greater than air. Therefore, its influence is negligible for our purposes.



(A) Free Fall

(B) Electric Field

**Figure 1: Free-body Diagram of Oil Droplets in Capacitor.** (a) When the droplet is undergoing free-fall due to gravity. (b) When the particle is under the influence of the uniform electric field.  $F_g$  is the force of gravity,  $F_v$  is the viscous drag force,  $F_b$  is the buoyancy force, and  $F_e$  is the electric field force.

$$\text{Gravitational } F_g = mg = \frac{4}{3}\pi a^3 \rho g \quad (1.1)$$

$$\text{Viscous Drag } F_v = 6\pi\eta a v_g \quad (1.2)$$

$$\text{Buoyancy } F_b = \frac{4}{3}\pi a^3 p_{air} g \quad (1.3)$$

$$\text{Electric } F_e = qE = q\left(\frac{V}{d}\right) \quad (2.1)$$

$$\text{Viscous Drag } F_v = 6\pi\eta a v_e \quad (2.2)$$

Where:

$m$  is the mass of the drop,

$g$  is acceleration due to gravity,

$a$  is the radius of the drop,

$\rho$  is the density of oil,

$\eta$  is the viscosity of air,

$v_g$  is the velocity in freefall,

$v$  is the fluid viscosity of the droplet,

$p_{air}$  is the density of the air,

$V$  is the voltage across the capacitor,

$d$  is the separation between the capacitor plates.

At equilibrium, the second law forces in equations (1) through (4) can be used to derive the charge of an electron as seen in equation (5), and the radius of a particle as seen in equation (6):

$$q = \frac{6\pi d \eta a}{v} (v_e + v_g) \quad (5)$$

$$a = \sqrt{\frac{9\eta v_g}{2g\rho}} \quad (6)$$

A limitation of this derivation is that Stokes' law does not hold for very small particles. Therefore, Millikan derived a correction factor which accounts for air pressure as seen in equation (7), where  $b$  the constant  $6.17 \cdot 10^{-6}$ , and  $p$  is the barometric pressure. This is the equation we will use for calculating charges.

$$q = \left(\frac{6\pi d}{v}\right) \left[\frac{9\eta^3}{2\rho g}\right]^{\frac{1}{2}} \left(1 + \frac{b}{pa}\right)^{-\frac{3}{2}} (v_e + v_g)(v_g)^{\frac{1}{2}} \quad (7)$$

## Experimental Methods

A diagram of the experimental apparatus can be seen in **Fig. 2**, where a camera views into the glass viewing port of a capacitor through a microscope. A preliminary measurement of components and independent variables is made. This includes the distances between capacitor plates  $d$ , the barometric pressure of the room  $p$ , the operating voltage across capacitor plates  $V$ . This is followed by a calibration of the apparatus, wherein the microscope and camera are adjusted so that a thin wire placed in the center of the capacitor is in focus. The capacitor is placed at a  $30^\circ$  angle with respect to the microscope, so that a light source applied through its back window is able to reflect off the particles but not obscure the image. In order to determine real distance within a video, a glass reference scale with divisions of a tenth of a millimeter is temporarily put in place of the capacitor and an image is taken. The distance between divisions is measured in pixels and a meter per pixel conversion factor is determined, allowing us to calculate velocity from pixel displacement per frame.

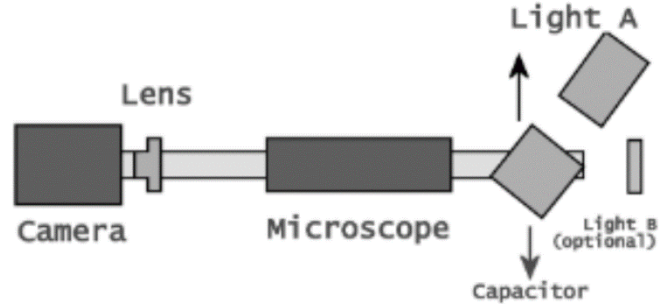


**Figure 2: Experimental Apparatus Configuration.**

A digital camera, microscope, and capacitor are fixed to a rail. The capacitor consists of two uniform metal plates parallel to Earth, with a hole in the top for injecting oil droplets, and two glass viewing ports on the sides. The top plate of the capacitor is connected to the positive terminal of a DC power supply and the bottom plate is connected to ground. A switchbox allows for a high positive voltage to be applied across the plates. The camera views into viewing port of a capacitor through the microscope as a light source is applied to the other viewing port in order to illuminate particles.

Once the calibration process is complete, the camera records as a mist of atomized oil droplets are injected through a hole in the top the capacitor where they undergo free-fall due to Earth's gravitational field. Once the lid is closed, a potential difference of 450 volts is applied across the capacitor plates from a DC power supply. The uniform electric field immediately causes positively charged particles to stick to the negatively charged plate, thereby lowering the density of unwanted particles within the system, which helps the tracker software identify desirable particles. The electric field is periodically turned off and on using a switch box, timed so that desirable particles are always within the frame of the video. This process is repeated for several cycles across several videos to increase the number of data points per particle. Each video is cut so that the electric field change occurs during the middle frame, allowing us to track particle velocity more accurately before and after the center point.

For the purpose of identifying and tracking single particle trajectories, we have written a custom program using *Trackpy*, a python package built around Crocker-Grier image processing algorithms<sup>[1]</sup> designed to track sub-micrometer spheres for the purposes of digital video microscopy. This allows us to simultaneously calculate the velocities of multiple particles to a subpixel precision of nanometers. The video is preprocessed with a band-pass which removes noise and background variation, and a threshold which separates the particles from the background. This allows the algorithm to locate particles through centroid peaks of particle width weighed over brightness. Various filtering methods allow us to characterize the neighborhoods of the peaks and take only those within a threshold of brightness, while discarding particles which exhibit undesirable behavior. For all remaining candidate particles, the program measures their trajectory in terms of pixel displacement and is able to determine their velocity using our defined meter per pixel scale and the framerate. For more information on the particle tracking process, see **Appx. A**.

## Results

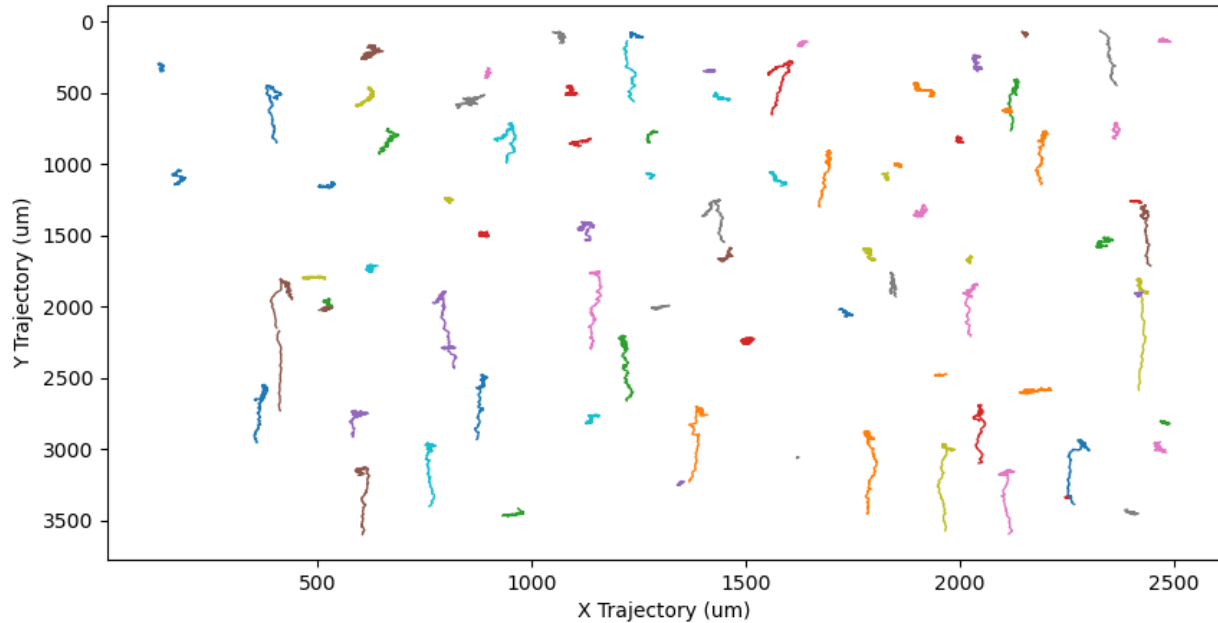


**Figure 3: Map of particle trajectory 250 frames before and after electric field change.** Both axes are distance in micrometers. The picture is inverted, where the negative direction in the Y-axis points towards the Earth. The X-axis is parallel to the capacitor plates. Long linear trajectories are characterized by displacement under the influence of the electric field where velocity is highest. These are desirable for measurement. The top point of these trajectory lines which travel in the opposite direction characterize displacement under free-fall. Smaller random trajectory paths are particles under heavy influence of Brownian motion and are undesirable for measurement.

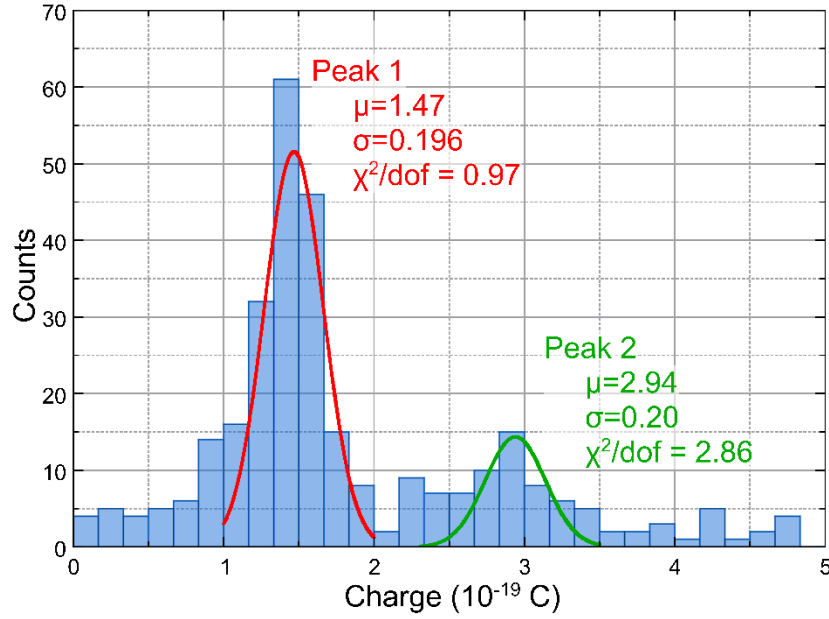


**Figure 4: Histogram of charges by particle count.** A histogram is made comprising of all 327 tracked particles sorted with a bin count of 30. Two distinct peaks are located at charges of  $1.47 \cdot 10^{-19}$  C (red) and  $2.94 \cdot 10^{-19}$  C (green) respectively. Peak 2 is an exact multiple of Peak 1, indicating quantization of charge. To the right of Peak 2, the next local maxima between 4 and 4.5 on the x-axis represents the charge  $4.41 \cdot 10^{-19}$  C, the third multiple of Peak 1.

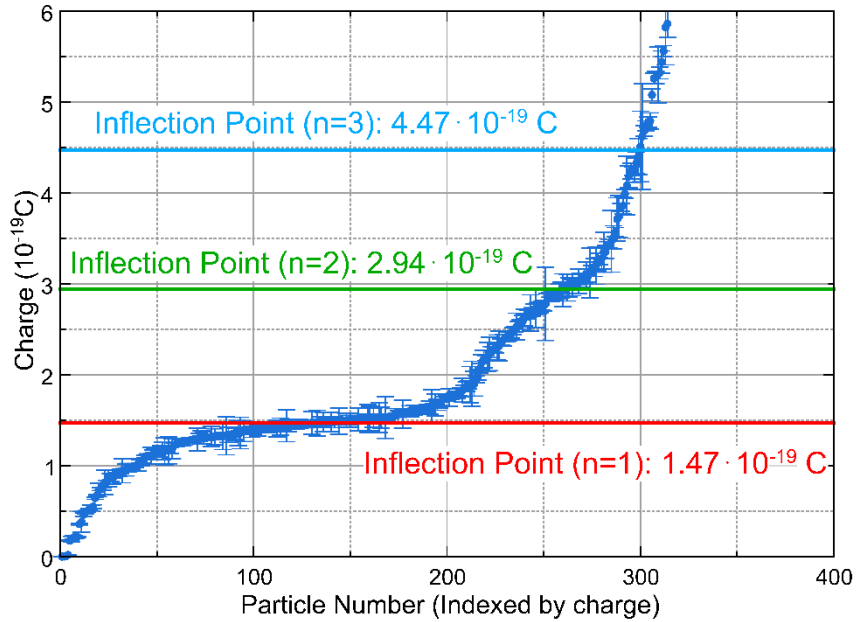


**Figure 5: Plot of particles sorted by charge.** Particle datapoints are characterized by blue dots with error caps in the y-axis. When sorting the particles by their charge there are distinct plateaus around factors of the base charge  $1.47 \cdot 10^{-19}$  C (red,  $n=1$ ). Particles between these inflection points are relatively few in number and exhibited amounts of Brownian motion which distort their velocities leading them to drift away from the charge factors. Charge factors of 2 (green) and 3 (blue) are clearly visible.

## Discussion and Conclusions

Between every video, the program identified features in the order of tens of thousands before any filtering was applied. Pre-processing filters refined positive identification of particles and post-processing filters removed those that did not change direction with 10 frames of the midpoint. Several other conditions were applied to ensure only particles which were desirable for measurement were added to the dataset; detailed information on this filtering process can be found in **Appx. A**. These techniques reduced the number of particles in the dataset to 327; the tracked trajectories of a small sample size can be seen in **Fig. 3**. A histogram of the charge distribution shows a clear trend towards multiples of the charge  $1.47 \cdot 10^{-19}$  C, as seen in **Fig. 4**. This charge factor can be quantized across the data as seen in **Fig. 5** when sorting particles by charge. The quantization of charge is clear as the datapoints trend towards multiples of the charge factor and their error bars do not account for overlapping between any other plateaus.

Ideally, to show quantization by charge the data should be discontinuous between these charge factors, but the effect of Brownian motion across a massive sample of particles influences the movement of each in varying levels of magnitude leading to spreads in data. There is a 8.59% difference in the charge factor we calculate as opposed to the accepted electron charge of  $1.602 \cdot 10^{-19}$  C. This is most likely due to limitations in how we can filter out irregularities in motion, shifting the overall trend away from the true charge.

In conducting the experiment there were a number of measurement errors identified, the biggest of which was in determining particle position. Given the low resolution of the video, particle diameters averaged around 10 pixels wide. Since the centroid often falls between pixels a prediction algorithm is used to determine its precise location, the uncertainty of which is the largest factor in charge error propagation<sup>[2]</sup>. For details on error propagation, see **Appx. B**. The distance between capacitor plates was measured using a caliper which was accurate to one hundredth of a millimeter. The voltage across the capacitor was measured using a voltmeter which could display four significant figures, giving an error of 0.05V. Mean sea-level pressure was taken from the Ohio State meteorological station and was corrected to the altitude of the campus and the temperature in the room in order to find barometric pressure. This value came out to be 73.82cm/Hg, which was similar to measurements taken using barometers within the room.

The majority of errors in this experiment are issues common in big data analysis, which can be improved by changing the way the experiment is approached. In terms of tracking particles, due to the sub-HD resolution of our camera, the program must use a larger degree of trajectory prediction to determine the location of a centroid between pixels. A camera with a higher resolution and framerate would improve the accuracy of velocity measurements. Regarding particle filtering in software, the random behavior of Brownian motion is generally left uncorrected, leaving a large spread of particles which were not ideal for measurement; seen in **Fig. 3**. Finer segmentation, filtering, and perhaps the assistance of machine learning would assist in removing particles which exhibit high amounts of Brownian motion and would therefore shift the data closer towards the quantized distribution. The tracking software could be improved to detect electric field changes by directional changes in velocity, which would allow for the tracking of individual particles between multiple cycles. Despite these problems, the data shows a clear trend towards the quantizability of electron charges.

## Citations

1. Crocker, J. C., & Grier, D. G. (1996). Methods of Digital Video Microscopy for Colloidal Studies. *J. Colloid Interf. Sci.*, 179(1), 298–310.
2. Thierry Savin, Patrick S. Doyle, Static and Dynamic Errors in Particle Tracking Microrheology, *Biophysical Journal*, Volume 88, Issue 1, 2005.

## Appendix A: Particle Filtering Techniques

The program finds particles by identifying small circular features within an image with a high contrast in brightness relative to the background. In order to differentiate between background and foreground, a bandpass filter is applied to the grayscale video. Once this is complete, particle filtering occurs in two stages, pre-processing filters which determine what the program will identify as a particle, and post-processing filters which remove particles from the dataset whose trajectories are undesirable. Particles which are desirable for measurement exhibit several measurable properties which we can utilize when it comes to these filtering techniques. Each filtering parameter is iteratively adjusted until an acceptable discrimination between desirable and undesirable particles is reached. In this experiment, approximately 1% of particles made it past both filtering processes and were used for calculating charge.

The pre-processing filters ensure we are only tracking particles which are clearly bright and isolated from any neighbors. The diameters in pixels of a small sample of particles in the desired range of focus are measured and this value is set as an upper threshold so that the program will only identify features which are smaller in size. A neighbor-separation threshold of twice the diameter is used to stop tracking a particle when it overlaps with another. Particles which meet these parameters can be seen in **Fig. A1**, denoted by red circles.

Once pre-processing analysis is complete, post-process filtering removes from the dataset any particles whose trajectories are undesirable. The program is able to track particles with sub-pixel accuracy by taking the average position of these pixels weighed by brightness. The uncertainty of this measurement in pixels is given by the program and used in propagating error in velocity. If the uncertainty in position is higher than one standard deviation of the mean, the particle is removed from the dataset. Additionally, particles that did not remain visible for more than four seconds were removed. In terms of behavior, desirable particles should be negatively charged, so any droplet which did not change its vertical direction when the electric field was applied was removed. Additionally, any particles whose velocity due to gravity  $v_g$  was of a larger in magnitude than their velocity under the influence of an electric field  $v_e$  was removed. Particles which exhibited large amounts of Brownian motion in the horizontal plane were undesirable as their random sporadic movements influence measurements of velocity. Therefore, any particles whose horizontal displacement was half as large as their vertical displacement were removed.

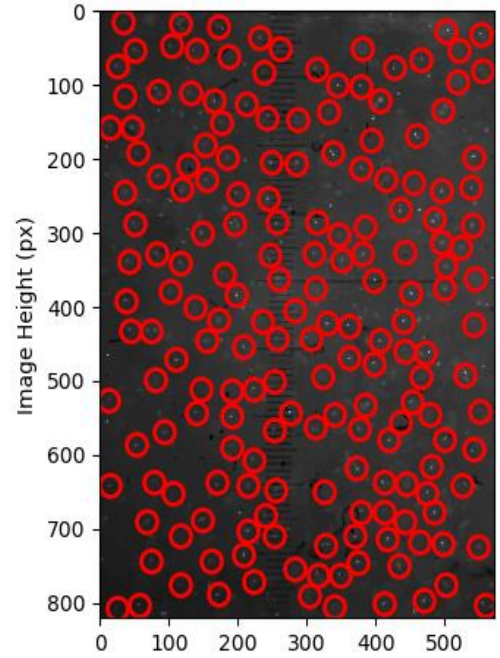


**Figure A1: Particles identified by the tracking algorithm.** Particles which meet the filtering parameters are identified, which is denoted by the red circles. For each frame, their pixel displacement is tracked and recorded.

## Appendix B: Error Propagation

Measurement	Value	Uncertainty	Uncertainty Rationale
Plate Distance	$3.897 \cdot 10^{-6} \text{ m}$	$\pm 4.41 \cdot 10^{-7}$	Caliper precision Plates not uniformly parallel
Oil Density (Nye watch oil)	$480 \text{ kg/m}^3$	-	Given by manufacturer
Viscosity of Air (20° C)	$1.825 \cdot 10^{-5} \text{ N} \cdot \text{s} \cdot \text{m}^{-2}$	-	Constant
Voltage	450V	$\pm 0.05$	Display limitations of voltmeter
Barometric Pressure	$73.82 \text{ cm} \cdot \text{Hg}^{-1}$	-	Gathered from weather station
Video Framerate	30.893 fps	0.447	Dropped frames
Meters per Pixel	$4.47 \cdot 10^{-6} \text{ m} \cdot \text{px}^{-1}$	$\pm 2.71 \cdot 10^{-8}$	Width of reference scale engravings

**Table B1: Measurements and their uncertainties**

Error in velocity was calculated with the uncertainty in meters per pixel (mpp) and the uncertainty in frame rate and propagating it alongside each individual particles uncertainty in position. The propagation for uncertainty in charge is shown in the equation below:

$$\Delta q = \sqrt{\left( \left( \frac{6\pi}{V} \sqrt{\frac{9\eta^3}{2\rho g}} \left( 1 + \frac{b}{Pr} \right)^{-\frac{3}{2}} (v_E + v_g) \sqrt{v_g} \Delta d \right)^2 + \left( \frac{6\pi d}{-V^2} \sqrt{\frac{9\eta^3}{2\rho g}} \left( 1 + \frac{b}{Pr} \right)^{-\frac{3}{2}} (v_E + v_g) \sqrt{v_g} \Delta V \right)^2 + \right. \\ \left. \left( \frac{6\pi d}{V} \sqrt{\frac{9\eta^3}{2\rho g}} \left( 1 + \frac{b}{Pr} \right)^{-\frac{3}{2}} \sqrt{v_g} \Delta v_E \right)^2 + \right. \\ \left. \left( \frac{27d \sqrt{\frac{\eta^3}{g\rho}} P^2 \sqrt{3\pi} \sqrt{3 + \frac{b \sqrt{\frac{2}{\pi}} \sqrt{\frac{g\rho}{\eta v_g}}}}{P}} \left( 3P \sqrt{2\pi} (3v_g + v_E) + b \sqrt{\frac{g\rho}{\eta v_1}} (9v_g + 5v_E) \right) \right)}{2V \left( 3P + b \sqrt{\frac{2}{\pi}} \sqrt{\frac{g\rho}{\eta v_g}} \right)^3 \sqrt{v_g}} \Delta v_g \right)^2} \right)^2}$$